COMPLETE DYNAMIC MODEL VALIDATION OF 3-DOF COMPLIANT MANIPULATOR WITH FLUIDIC MUSCLES

TOMAS CAKURDA, MONIKA TROJANOVA, ALEXANDER HOSOVSKY

Technical University of Kosice, Faculty of Manufacturing Technologies with the Seat in Presov, Slovakia

DOI: 10.17973/MMSJ.2022_12_2022135

monika.trojanova@tuke.sk

The article is devoted to the description of the validation of the dynamic model of an angular manipulator with three degrees of freedom of movement based on the chosen course of excitation of pneumatic artificial muscles from the manufacturer FESTO. The dynamic model consists of the dynamics of the manipulator arm and the dynamics of the pneumatic part of the experimental system. The motion equations were derived based on Lagrangian formalism and the dynamic of muscle contraction can be described using Newton's second law. The overall model of the system was implemented in the Matlab Simulink environment. The outputs of the validations were compared with the measured data from the real system. The observed parameter was the angle of rotation of the joint. Two statistical indicators were used to compare the simulation outputs (model) with the system outputs (measurements), namely NRMSE (Normal Root Mean Square Error) and MAE (Mean Absolute Error).

KEYWORDS

Dynamics, Lagrangian formalism, Fluid Muscle, Angular robotics arm, Validation

1 INTRODUCTION

Traditional robotics has undergone a fundamental paradigm shift in recent decades, both in research and development, but also in real applications. Initially, industry was dominated by potentially dangerous rigid robots that perform typical automation tasks without humans in their immediate vicinity. Robots use rigid drives and elastic deformation in their transmission system is considered undesirable. The development of industry, medicine and the increasing demands of society have triggered the need to develop a new generation of safe robots of light construction that exceed the capabilities of existing industrial robots. Robots are expected to work in close proximity to humans or in collaboration with humans in dynamic conditions where the work environment is unknown and changeable. The ability to perceive physical interaction, plan movements and cooperate with people in mind, represents new application possibilities and progress in the field of safe and seamless human-robot interaction. [Albu-Schaffer 2016]

Artificial muscle technology is a highly interdisciplinary field of research that overlaps with various fields such as materials science, chemical engineering, mechanical engineering, electrical engineering, and chemistry. Simulating muscle-generated movements such as moving, lifting, turning, and bending presents interesting application possibilities in robotics and electromechanical systems. Artificial muscle is a general term for a class of materials and devices that can reversibly contract, rotate, or expand as a result of an external stimulus (such as voltage, current, pressure, temperature, light, etc.). The three basic reactions to compression (contraction, expansion, and rotation) can be combined within a single component to create other types of motion (eg, bending, contracting one side of the material and expanding the other side). [Mirvakili 2018]

Effective use of robots in various applications of industrial production and safe human-robot interaction is currently an important aspect of robotics research. The desired movement of the robot or manipulator is based on a detailed description of their individual properties, the derivation of kinematic and dynamic models or a complex process of simulating their movement. The required control of the manipulator is based on the correct description of the real system in the form of its model. The authors deal with the issues of kinematic and dynamic modeling of systems in the publications [Siciliano 2016] and [Kurfess 2018].

Dynamic modeling was used to describe the behavior of the investigated system (experimental manipulator), which serves to determine the basic relationship between force and movement of the respective system. Within dynamic modeling, the system model can be derived based on two basic principles described in [Spong 2020], namely the Euler-Lagrange formulation (the system is described as a whole based on the difference in kinetic and potential energy) and the Newton-Euler formulation (the derivation of the dynamic model is more demanding as each member of the system is described separately). The selection of the method takes into account aspects such as the number of degrees of freedom, joint spacing and others. [Trojanova 2021]. The authors of the article [Al-Shuka 2019] used the Euler-Lagrange formulation and the Newton-Euler formulation to derive the motion equations of a biped robot during different phases of walking. In another work [Azar 2022], use the Euler-Lagrange formulation to derive a dynamic model of a two-link robotic manipulator.

In order to obtain a complete dynamic model, it was also necessary to derive a drive model. Unlike commonly used actuators in robotic applications, pneumatic artificial muscles have specific properties that complicate their modeling and control. The authors of the article [Kalita 2022] deal with the basic issue of pneumatic artificial muscles. The dynamics of muscle contraction is expressed using Newton's second law. For the derivation of the dynamics, the publication [Hosovsky 2016] was used, where the authors deal with the dynamic characterization and simulation of a two-link soft robot arm with pneumatic muscles. Lagrangian formalism was also used to create a dynamic model in publications [Trojanova 2020]. The investigated system is a planar robotic arm with two degrees of freedom of movement.

With the progress of research in the given issue, the dynamics of an experimental manipulator with three degrees of freedom based on the Lagrangian formalism, which considers the difference between the kinetic and potential energy of the system, is described in the corresponding article. The mathematical model was implemented in the Matlab Simulink environment. The created model (diagram) was used for subsequent simulations - the validation process. The main goal of the research described in the article is the derivation of a dynamic model for an angular mechanism with three degrees of freedom and the subsequent validation of the model, which was to test the functioning and accuracy of the model based on the comparison of simulation outputs and measured data from the

real system. The article is divided into 6 chapters. After the introduction, the second chapter deals with the description of the experimental manipulator. In the third chapter, the dynamic model of the system is defined. The fourth chapter presents the measured data, and the fifth chapter presents the validation results from the Matlab Simulink environment. The last chapter provides a summary of the concerned research.

2 EXPERIMENTAL SETUP

The subject of the research is an angular robotic arm with three degrees of freedom of movement shown on Figure 1. The movement of the arm is ensured by means of pneumatic artificial muscles in an antagonistic connection. The researched experimental manipulator was designed and constructed at the workplace of the authors for the purposes of research into actuation based on artificial muscles.

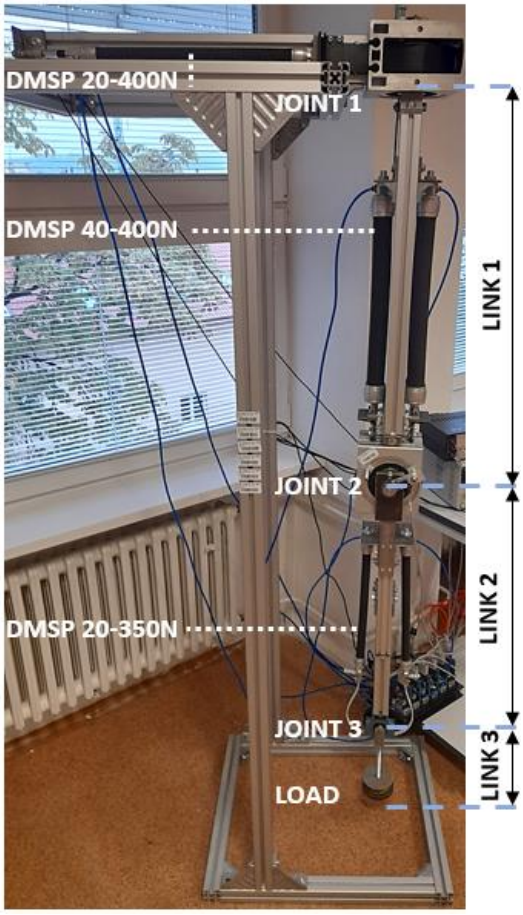

Figure 1. Experimental manipulator

The experimental manipulator consists of a support construction and an arm. The construction of the manipulator is represented by aluminum profiles forming the lower, upper base, stand and links of the manipulator. The arm consists of three rotary joints and three links. The actuation of the arm is ensured by three pairs of pneumatic artificial muscles from the manufacturer FESTO in an antagonistic connection. Joint 1 is driven by a pair of muscles FESTO DMSP 20-400N-RM-CM, Joint 2 by a pair of muscles FESTO DMSP 40-400N-RM-CM and Joint 3 by a pair of muscles FESTO DMSP 20-350N-RM-CM. The principle of operation of the drive of pneumatic artificial muscles consists in their contractions, which occur when the muscle is pressurized by the working medium (compressed air). During the contraction of the muscle, a tensile force is created, and based on their antagonistic connection and the pulley-toothed belt subsystem, results in a rotational movement. The individual components thus ensure the transmission of the torque. The supply of compressed air is provided by the AIRSTAR AC 401/50 compressor, and the pressure in individual muscles is regulated using MATRIX ERP50 pressure regulators, which also contain muscle pressure sensors. The KORAD KD3005D is used as a source, and the control of the arm is provided using the Matlab Simulink program. Control signals are processed by the I/O PCI card Humusoft MF624.

3 DYNAMIC MODEL OF THE SYSTEM

The experimental manipulator represents one of the basic kinematic structures, namely an angular arm with three rotating joints. The diagram of the kinematic structure is shown in Figure 2. It serves to show the basic elements of the manipulator, their location within the entire system, but also to indicate the basic parameters. An overview of the parameters used in the diagram, but also the mathematical formulation, is contained in Table 1.

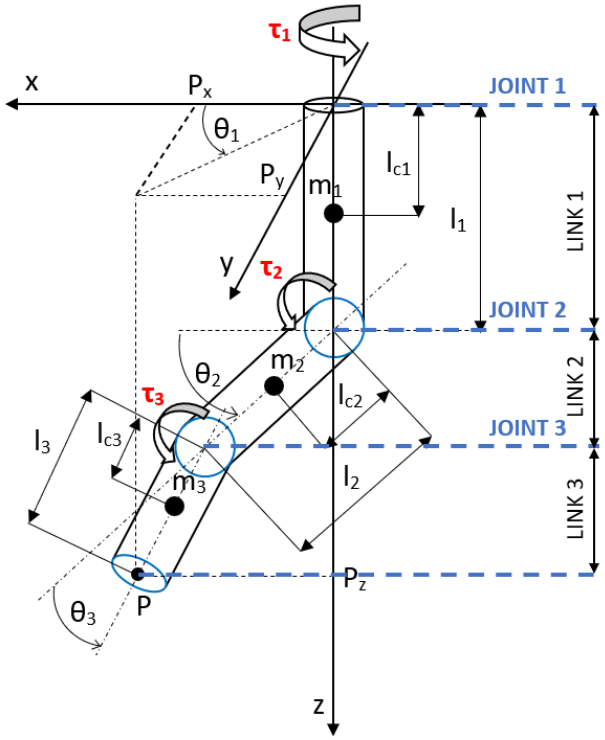

Figure 2. The scheme of angular robotic arm with 3-DOF

$\theta_1, \theta_2, \theta_3$	Joint 1, 2, 3 angle
m_1, m_2, m_3	Link 1, 2, 3 mass
l_1, l_2, l_3	Link 1, 2, 3 length
l_{c1}, l_{c2}, l_{c2}	Link 1, 2, 3 center of mass
τ_1, τ_2, τ_3	Joint 1, 2, 3 generalized force
I_{x2}, I_{x3}	Link 2, 3 moment of inertia about axis x
I_{y2}, I_{y3}	Link 2, 3 moment of inertia about axis y
I_{z1}, I_{z2}, I_{z3}	Link 1, 2, 3 moment of inertia about axis z
g	Gravity constant

Table 1. Overview of parameters listed in the dynamic model

3.1 *Manipulator arm dynamic*

The dynamic model of the described system was derived using Lagrange's equations. The Lagrangian equations for a 3 degree

of freedom manipulator are generally given in Equation 1 [Kelly 2005], where L is the Lagrangian, φ_i is the joint position, derivation of the joint position is joint velocities, and τ_i is the force term.

$$\frac{d}{dt}\left[\frac{\partial L}{\partial \dot{\varphi}_i}\right] - \frac{\partial L}{\partial \varphi_i} = \tau_i \qquad i = 1,2,3 \tag{1}$$

By calculating the Lagrangian and applying Equation 1, we get three nonlinear differential equations that represent the dynamics equations of the described manipulator. For Link 1, 2 and 3, the force components τ_1, τ_2 and τ_3 are determined in the final form consciously in Equation 2, Equation 3 and Equation 4. [Murray 1994]

$$\begin{aligned}\tau_1 = {} & \left[\left(I_{y2} - I_{z2} - m_2 l_{c2}^2\right)c_2 s_2 + \left(I_{y3} - I_{z3}\right)c_{23}s_{23} - m_3(l_2 c_2 + l_{c3}c_{23})(l_2 s_2 + l_{c3}s_{23})\right]\dot{\theta}_1\dot{\theta}_2 + \left[\left(I_{y2} - I_{z2} - m_2 l_{c2}^2\right)c_2 s_2 + \left(I_{y3} - I_{z3}\right)c_{23}s_{23} - m_3(l_2 c_2 + l_{c3}c_{23})(l_2 s_2 + l_{c3}s_{23})\right]\dot{\theta}_1\dot{\theta}_2 + \left[\left(I_{y3} - I_{z3}\right)c_{23}s_{23} - m_3 l_{c3}s_{23}(l_2 c_2 + l_{c3}c_{23})\right]\dot{\theta}_1\dot{\theta}_3 + \left[\left(I_{y3} - I_{z3}\right)c_{23}s_{23} - m_3 l_{c3}s_{23}(l_2 c_2 + l_{c3}c_{23})\right]\dot{\theta}_1\theta_3 + \left[I_{y2}s_2^2 + I_{y3}s_{23}^2 + I_{z1} + I_{z2}c_2^2 + I_{z3}c_{23}^2 + m_2 l_{c2}^2 c_2^2 + m_3(l_2 c_2 + l_{c3}c_{23})^2\right]\end{aligned} \tag{2}$$

$$\begin{aligned}\tau_2 = {} & [I_{x3} + m_3 l_{c3}^2 + m_3 l_2 l_{c3}c_3]\ddot{\theta}_3 + \left[\left(I_{z2} - I_{y2} + m_2 l_{c2}^2\right)c_2 s_2 + \left(I_{z3} - I_{y3}\right)c_{23}s_{23} + m_3(l_2 c_2 + l_{c3}c_{23})(l_2 s_2 + l_{c3}s_{23})\right]\dot{\theta}_1^2 - [l_2 m_3 l_{c3}s_3]\dot{\theta}_2\dot{\theta}_3 - [l_2 m_3 l_{c3}s_3]\dot{\theta}_2\dot{\theta}_3 - [l_2 m_3 l_{c3}s_3]\dot{\theta}_3^2 + [I_{x2} + I_{x3} + m_3 l_2^2 + m_2 l_{c2}^2 + m_3 l_{c3}^2 + 2m_3 l_2 l_{c3}c_3] - (m_2 g l_{c2} + m_3 g l_2)c_2 - m_3 l_{c3}c_{23}\end{aligned} \tag{3}$$

$$\tau_3 = [I_{x3} + m_3 l_{c3}^2 + m_3 l_2 l_{c3}c_3]\ddot{\theta}_2 + \left[\left(I_{z3} - I_{y3}\right)c_{23}s_{23} + m_3 l_{c3}s_{23}(l_2 c_2 + l_{c3}c_{23})\right]\dot{\theta}_1^2 + l_2 m_3 l_{c3}s_3\dot{\theta}_2 + (I_{x3} + m_3 l_{c3}^2) - m_3 g l_{c3}c_{23} \tag{4}$$

The dynamic model of the experimental manipulator expressed in Equation 2, Equation 3 and Equation 4 can be written in a compact form by Equation 5 [Ashagrie 2021]. The relevant formulation needs to be supplemented with a friction component, which represents friction in the joints during links movement. The final form of the Lagrangian dynamic model is expressed by Equation 6 [Ashagrie 2021]. The friction force $\mathrm{F}(\dot{\theta})$ is defined by Equation 7, where used friction model is based on the extended Coulomb model [Liu 2015]. It might include the Stribeck effect, and it may assume the following polynomial form, which is a generalization of the Coulomb and viscous model. Constants f_{ci}, f_{di}, f_{ei}, f_{gi} where i = 1, 2, 3 are parameters obtained with a identification and $\dot{\theta}$ is the angular velocity. [Lei 2021]

$$M(\theta)\ddot{\theta} + C\left(\theta,\dot{\theta}\right)\dot{\theta} + G(\theta) = \tau \tag{5}$$

$$M(\theta)\ddot{\theta} + C\left(\theta,\dot{\theta}\right)\dot{\theta} + G(\theta) + F\left(\dot{\theta}\right) = \tau \tag{6}$$

$$F\left(\dot{\theta}\right) = f_{ci}sgn\left(\dot{\theta}\right) + f_{di}\dot{\theta} + f_{ei}\dot{\theta}^2 sgn\left(\dot{\theta}\right) + f_{gi}\dot{\theta}^3 \tag{7}$$

3.2 Actuator dynamics

For the derivation of a complete dynamic model of the experimental manipulator, we have to derive also dynamic model of actuators. The dynamic of muscle contraction can be described using Newton's second law by Equation 8 [Hosovsky 2016]:

$$m\ddot{y} + F_D\left(\dot{\zeta},P_m\right) + F_S(\zeta,P_m) = F_e - F_g \tag{8}$$

where m – moved mass [kg], y – muscle displacement [m], $F_D\left(\dot{\zeta},P_m\right)$ – nonlinear damper force [N], $F_S(\zeta,P_m)$ – nonlinear spring force [N], P_m - muscle pressure [kPa], ζ – muscle contraction [%], F_e – external (opposing) muscle force [N] and F_g is gravity force [N]. One rotary joint driven by a pair of PAMs under the influence of gravity can be seen as two parallel connections of a nonlinear spring and damper with one spring-damper system acting against gravity and the other supplying gravity. Then can be written Equation 9 and Equation 10 for muscles movement. These equations are applied in the movement of Joint 2 and Joint 3. In the case of Joint 1 the effect of gravity is not considered. [Pitel 2013]

$$m\ddot{y}_1 + F_{D1}\left(\dot{\zeta},P_m\right) + F_{S1}(\zeta,P_m) = F_{D2}\left(\dot{\zeta},P_m\right) + F_{S2}(\zeta,P_m) + F_g \tag{9}$$

$$m\ddot{y}_2 + F_{D2}\left(\dot{\zeta},P_m\right) + F_{S2}(\zeta,P_m) = F_{D1}\left(\dot{\zeta},P_m\right) + F_{S1}(\zeta,P_m) - F_g \tag{10}$$

The nonlinear spring force term corresponds to a static force function of PAM that depends on muscle pressure and its contraction and which is commonly identified from the experimental data. This function was approximated using MLP (A multilayer perceptron - a feedforward network of simple neurons that maps sets of input data onto a set of outputs). Based on a linear combination of the real inputs, the perceptron calculates the output using a non-linear activation function (Equation 11), where w is weights vector, x is the input vector, b is the bias, and φ represents the activation function. As the activation function MLP system use hyperbolic tangent. The mathematical formula for the approximated function is then given by the Equation 12. [Awad 2015]

$$y = \varphi(z) = \varphi\left(\sum_{i=1}^{n} w_i x_i + b\right) \tag{11}$$

$$y = \varphi(z) = \tanh(z) = \frac{2}{(1 + e^{-2z})^{-1}} \tag{12}$$

In Matlab Simulink was used an MLP network with one hidden layer and ten neurons was for muscles with a diameter of 40 mm and an MLP network with one hidden layer and thirty neurons for muscles with a diameter of 20 mm. For the nonlinear damper force term, were used a relationship where the force is directly proportional to the product of muscle pressure and muscle contraction velocity (Equation 13), where μ is a damping coefficient [m²·s].

$$F_D\left(\dot{\zeta},P_m\right) = \mu P_m\dot{\zeta} \tag{13}$$

Because both nonlinear terms in Equation 8 directly depend on the muscle pressure, it is also necessary to describe the dynamics of the pneumatic part of the PAM to obtain its behavior in time. Assuming an ideal gas confined to a closed space, the time derivative of the PAM pressure can be derived using the Boyle-Marriott law, which states that the product of the gas pressure and its volume is constant if the temperature in the closed system does not change. This terms is given in Equation 14, where P_a – atmospheric pressure [Pa], V_a – volume of compressed air within muscle [m³], P_m – absolute muscle pressure [Pa] and V_m – muscle volume [m³]. Solving for P_m and taking the time derivative gives Equation 15. [Tipler 2007], [Hosovsky 2016]

$$P_a V_a = P_m V_m \tag{14}$$

$$\dot{P}_m = P_a\frac{\dot{V}_a}{V_m} - P_m\frac{\dot{V}_m}{V_m} \tag{15}$$

To complete Equation 15, it is necessary to determine the volume of the muscles $V_m(\zeta)$ given by Equation 16. The time rate of change of muscle volume $\dot{V}_m\left(\zeta,\dot{\zeta}\right)$ expressed by Equation 17. This equation is given by time derivate of Equation 16. [Hosovsky 2016]

$$V_m(\zeta) = a_1\zeta^3 + a_2\zeta^2 + a_3\zeta + a_4 \tag{16}$$

$$\dot{V}_m\left(\zeta,\dot{\zeta}\right) = 3a_1\zeta^2\dot{\zeta} + 2a_2\zeta\dot{\zeta} + a_3\dot{\zeta} \tag{17}$$

We used n = 3 and the following values of polynomial coefficients determined using Curve Fitting Toolbox in Matlab. The coefficient values for individual muscle volumes are shown in Table 2.

	20-400N	40-400N	20-350N
a_1	-1.778*10^{-3}	-1.538*10^{-2}	-1.543*10^{-3}
a_2	1.583*10^{-5}	1.581*10^{-3}	-5.312*10^{-7}
a_3	7.815*10^{-4}	2.994*10^{-3}	6.832*10^{-4}
a_4	1.256*10^{-4}	5.036*10^{-4}	1.099*10^{-4}

Table 2. Values of polynomial coefficients

The volume air flow through a valve which describes $\dot{V}_a$, expressed by Equation 18 and Equation 19, represent the last term that needs to be defined to complete the muscle pressure dynamics model. This model expresses the mass flow using two valve parameters which are sonic conductance and critical ratio [Beater 2007], [Hosovsky 2016]:

$$\dot{V}_a = P_1 C \sqrt{\frac{T_0}{T_1}} \sqrt{1 - \left(\frac{\frac{P_2}{P_1} - b}{1 - b}\right)^2}, if\ \frac{P_2}{P_1} > b \tag{18}$$

$$\dot{V}_a = P_1 C \sqrt{\frac{T_0}{T_1}}, if\ \frac{P_2}{P_1} \leq b \tag{19}$$

where P_1 is upstream pressure [Pa], P_2 is downstream pressure [Pa], T_0 – temperature of air at reference conditions [K], T_1 – upstream temperature of air [K], b – critical ratio [–], C – sonic conductance [m^3·s^{-1}·Pa^{-1}].

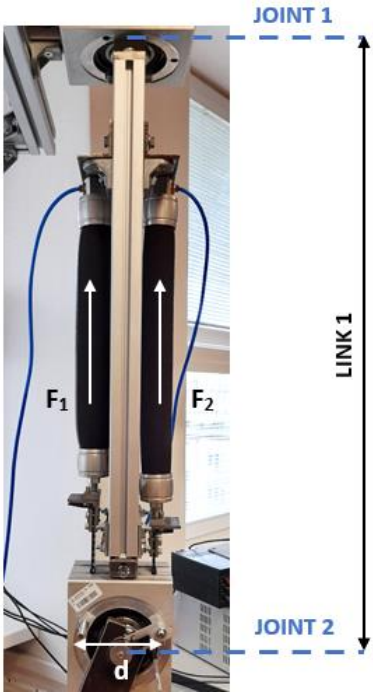

Figure 3. Muscles forces for Link 1 of 3-DOF robotic arm

When driving rotational joints, we consider the torque developed by a pair of pneumatic artificial muscles. In this case, the gravity is manifested through torques that need to be compensated by the muscles. From Equation 8 we can observed that the muscle contraction dynamics depend on two nonlinear terms corresponding to nonlinear spring force and nonlinear damper force. Then is torque expressed by Equation 20, where F_1, F_2 are muscles forces and d is sprocket diameter. The direction of effect of the forces is shown on Figure 3.

$$\tau = (F_1 - F_2) * d/2 \tag{20}$$

At steady-state and with respect to Equation 20, the muscles must generate a force difference to compensate for the torque due to gravity. The relevant forms are given in Equation 21 and Equation 22, where $k = g/r$ and g – gravity constant [m·s^{-2}] and r – sprocket diameter [m]. [Hosovsky 2016]

$$\Delta F_1 = [(m_3 * l_2 + m_2 * l_{c2})cos\theta_2 + m_3 l_{c3} cos(\theta_2 + \theta_3)]k \tag{21}$$

$$\Delta F_2 = m_3 l_{c3} cos(\theta_2 + \theta_3)k \tag{22}$$

4 MEASURED DATA

The data necessary for the subsequent validation of the model were obtained based on muscle excitation using the control signals of the Signal Builder tool of the Matlab Simulink program. During the measurements, an initial pressure value of 550 kPa was chosen for individual muscles, and for specified time intervals, one of the pair of muscles was subsequently deflated by a certain value of pressure in the muscle and again pressurized to a value of 550 kPa. The purpose of the measurements was to obtain the waveforms of the monitored output parameter – the Joint angle of the manipulator's arm. The total number of measurements for the selected method of muscle excitation was 10, and the courses of these measurements were subsequently averaged. The total measurement time was set at 120 seconds.

For the upper pair of muscles that drives Joint 1, the value of the pressure by which one and then the other muscle is deflated in the given interval was chosen to 350 kPa. The course of the control signals for the right and left muscles is presented in Figure 4. The average course of pressure values in the muscles are shown in the Figure 5.

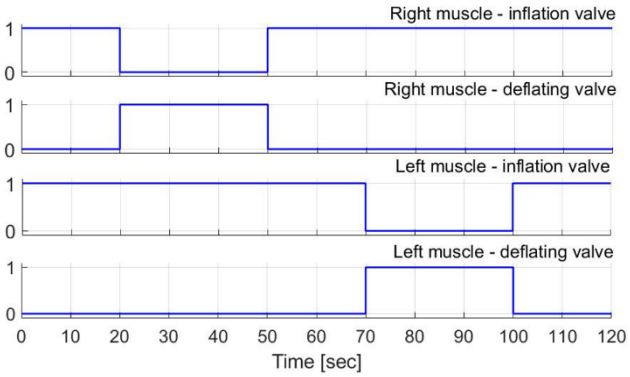

Figure 4. Control signals for a pair of muscles of Joint 1

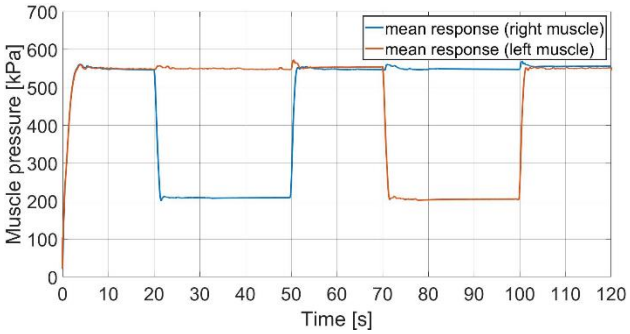

Figure 5. Response of mean pressure in muscles for Joint 1

The value of the pressure by which the muscles of Joint 2 were deflated was 250 kPa. Figure 6 shows the corresponding control signals. The average course of pressure values in the muscles are shown in the Figure 7.

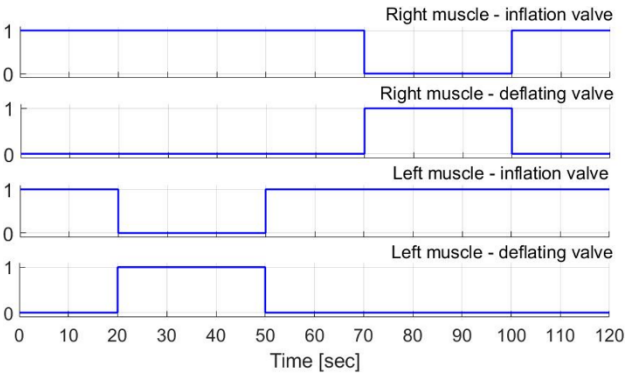

Figure 6. Control signals for a pair of muscle of Joint 2

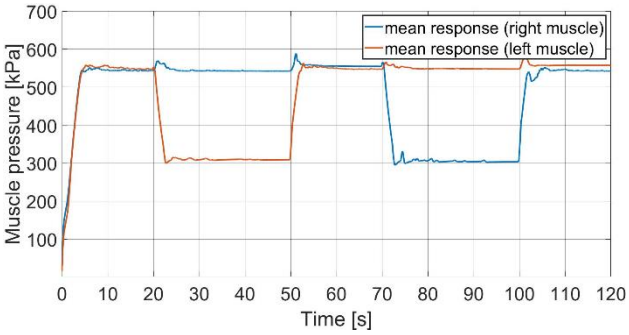

Figure 7. Response of mean pressure in muscles for Joint 2

The third lower pair of muscles for Joint 3 was deflated by 450 kPa. The control signals are shown in Figure 8. Figure 9 shows the pressures in the lower pair of pneumatic artificial muscles based on the selected excitation signal.

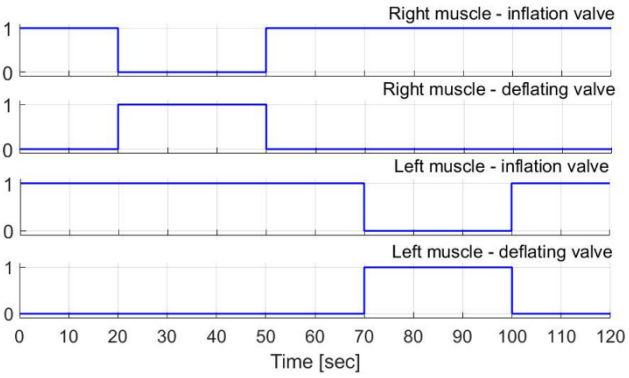

Figure 8. Control signals for a pair of muscles of Joint 3

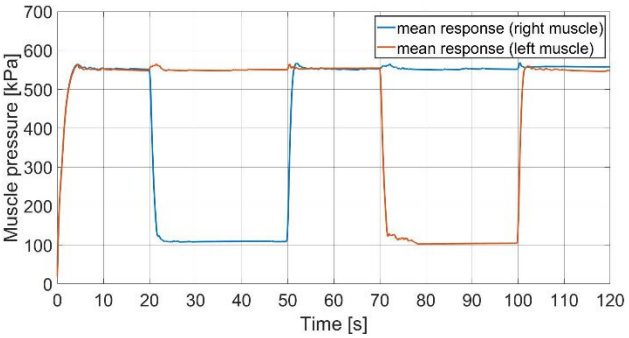

Figure 9. Response of mean pressure in muscles for Joint 3

The average course of the output monitored parameter determined on the basis of the measurements made using the drive by pneumatic artificial muscles is shown in the Figure 10, Figure 11 and Figure 12. The size of the angle of deviation of individual links depends on the pressure value by which the corresponding muscle is deflated while maintaining the determinated pressure value of the other muscle. With the increasing value by which the muscle is deflated, the size of the deflection of the links also increases.

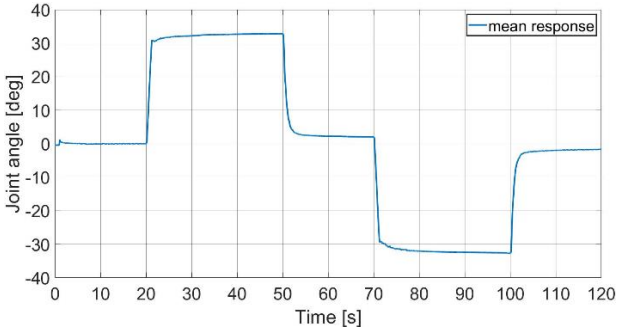

Figure 10. Response of mean measured angle for Link 1

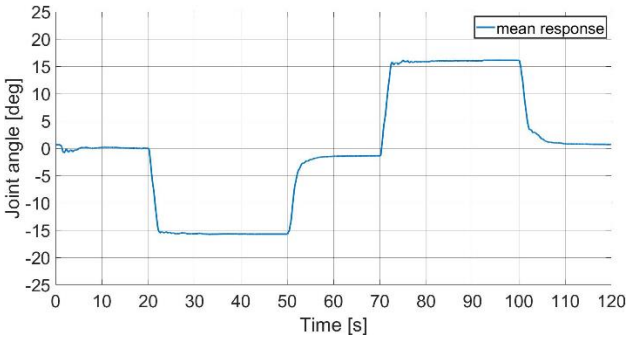

Figure 11. Response of mean measured angle for Link 2

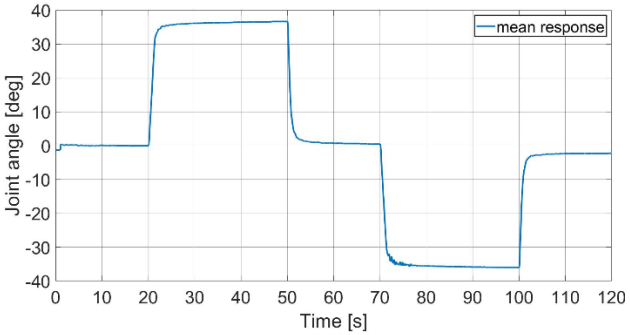

Figure 12. Response of mean measured angle for Link 3

5 RESULTS OF VALIDATION FROM SIMULINK

For the purposes of validation, a scheme was created in the Matlab Simulink environment that represents the dynamic model of the real system described in the chapter entitled Dynamic Model of The System. The basic physical parameters of the system were exported from the CAD software, which was used to make a 3D model of the system. The individual constants for the respective friction model were obtained by identification. Designations, values and units of input parameters are given in Table 3 and Table 4. A simulation was performed, while its time was identical to the time of measurements.

Designation	Value	Unit
I_{x2}	0.0514	kg.m^2
I_{x3}	0.0661	kg.m^2
I_{y2}	0.0037	kg.m^2
I_{y3}	0.0003	kg.m^2
I_{z1}	0.0037	kg.m^2
I_{z2}	0.0036	kg.m^2

Table 3. Overview of values of input parameters of Simulink model – part 1.

Designation	Value	Unit
I_{z3}	0.0003	kg.m^2
l	0.8099	m
m_2	11.7805	kg
m_3	4.8147	kg
l_{c2}	0.5550	m
l_{c3}	0.1910	m
f_{c1}	0.2082	N.m.s.rad^{-1}
f_{d1}	0.1322	N.m
f_{e1}	0.5148	N.m.s.rad^{-1}
f_{g1}	7.7218	N.m
f_{c2}	0.1956	N.m.s.rad^{-1}
f_{d2}	0.0349	N.m
f_{e2}	0.0532	N.m.s.rad^{-1}
f_{g2}	0.2263	N.m
f_{c3}	0.0524	N.m.s.rad^{-1}
f_{d3}	0.0176	N.m
f_{e3}	0.4850	N.m.s.rad^{-1}
f_{g3}	0.3041	N.m
b	0.4330	-
C	12.2891	m^3·s^{-1}·Pa^{-1}

Table 4. Overview of values of input parameters of Simulink model – part 2.

The outputs of the validation are matrices exported from the Simulink environment to the Matlab environment. The exported outputs of the simulations were compared with the data waveforms processed from the measured data. To compare the simulation outputs (model) with the system outputs (measurements) were used two statistical indicators, namely NRMSE (Normal Root Mean Square Error) and MAE (Mean Absolute Error). NRMSE compares the degree of agreement of the simulated output with the measured data. The mathematical formulation of NRMSE is given in Equation 23, where y_j is system output on the k-th sample, $\hat{y}_j$ represents model output on the k-th sample and n is number of samples. The desired value is for NRMSE = 100%, when the model and system output are identic. The MAE indicator is based on a numerical value, represents the size of the error created during the simulation compared to the measured values (Equation 24). [Trojanova 2021]

$$NRMSE = \left(1 - \frac{\sqrt{\sum_{j=1}^{n}\left[y_j - \hat{y}_j\right]^2}}{\sqrt{\sum_{j=1}^{n}\left[y_j - \frac{1}{n}\sum_{j=1}^{n} y_j\right]^2}}\right) \times 100\% \quad (23)$$

$$MAE = \frac{1}{n}\sum_{j=1}^{n}\left|y_j - \hat{y}_j\right| \quad (24)$$

5.1 *Muscle dynamics model validation*

In the first test was performed the validation of the pneumatic part of the dynamic model of the experimental manipulator. The pattern of the excitation signal of the simulation corresponded to the description from the previous chapter. The validation results based on the selected criteria for individual pairs of muscles are shown in the Table 5. The value of the statistical indicator NRMSE was around 90%. The highest was for the left muscle of Link 3, specifically 91.14%, and the lowest for the right muscle of Link 2, inde 86.93%.

Link 1			
Right muscle		**Left muscle**	
NRMSE	90.52 %	NRMSE	90.77 %
MAE	7.0587	MAE	5.2831
Link 2			
Right muscle		**Left muscle**	
NRMSE	86.93 %	NRMSE	89.13 %
MAE	9.3672	MAE	7.7046
Link 3			
Right muscle		**Left muscle**	
NRMSE	90.72 %	NRMSE	91.14 %
MAE	8.7856	MAE	6.8563

Table 5. Overview of results of validation based on criteria NRMSE and MAE for single links

Comparing the simulation outputs, scheme of the pneumatic part of the dynamic model of the experimental manipulator, pointed out that the pneumatic part is modeled very well. The model is able to satisfactorily simulate real pressurization and de-pressurization of muscles with minor deviations from the real system. A comparison of the pressure curves of individual muscles is shown in the Figure 13, Figure 14 and Figure 15. The main purpose of validation the pneumatic part by pressurizing and depressurizing all muscles was to find out if there is a significant asymmetry associated with the pneumatic configuration of the system. The source of deviations between individual courses can be errors in the modeling of airflow dynamics, as well as the dependence of the muscle volume on contraction and its time derivative.

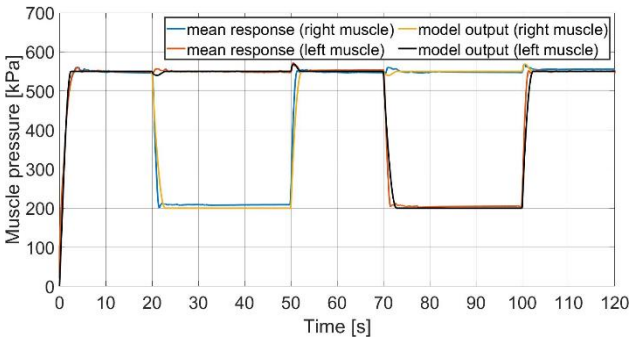

Figure 13. Model output of validation for the Link 1

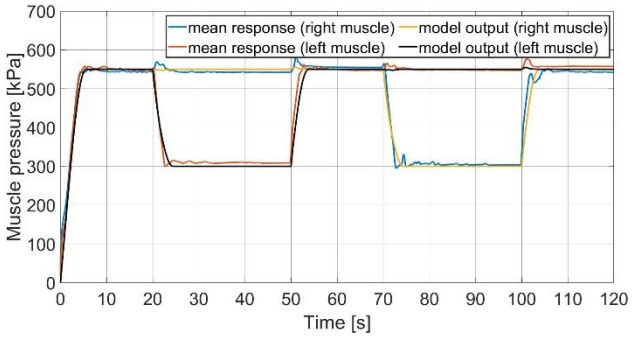

Figure 14. Model output of validation for the Link 2

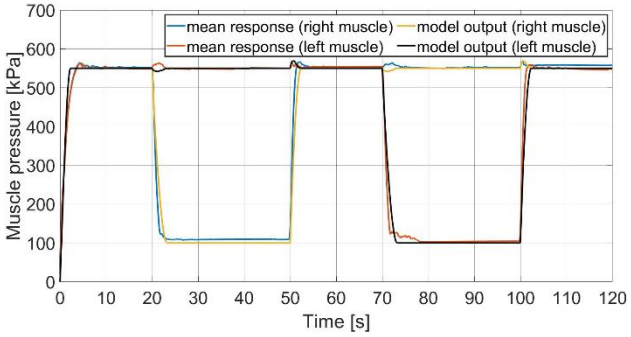

Figure 15. Model output of validation for the Link 3

5.2 *Complete model validation*

In the second test was performed the validation of the complete dynamic model of the experimental manipulator. Validation of the model was carried out with the simultaneous drive of all joints. The course of control signals and pressure values for individual muscles are identical to the description from the previous chapter. The compared parameter was the size of the deflection angle of individual links. The validation results based on the selected criteria for individual links are shown in the Table 6. The best value of the statistical indicator NRMSE was for the deviation of Link 1, namely 93.33% and the lowest for the deviation of Link 2, inde 82.02%. This value follows the lower values of the NRMSE indicator in the validation of the pneumatic part of the model for Link 2.

Link 1	NRMSE	93.33 %
	MAE	1.0046
Link 2	NRMSE	82.02 %
	MAE	1.4564
Link 3	NRMSE	92.34 %
	MAE	1.4377

Table 6. Overview of results of validation based on criteria NRMSE and MAE for single links - Complete model validation

A comparison of the simulation outputs, the scheme of the dynamic model of the investigated manipulator pointed out that the deflection of the links using pneumatic artificial muscles is modeled at a sufficient level. The model is able to satisfactorily simulate the movement of the links manipulator with minor deviations from the real system. A comparison of the measured curves and the simulation outputs is in Figure 16, Figure 17 and Figure 18. As a whole, the model captures the nature of the system dynamics, taking into account the interaction between the drive and the manipulator arm as well as the individual joints of the arm.

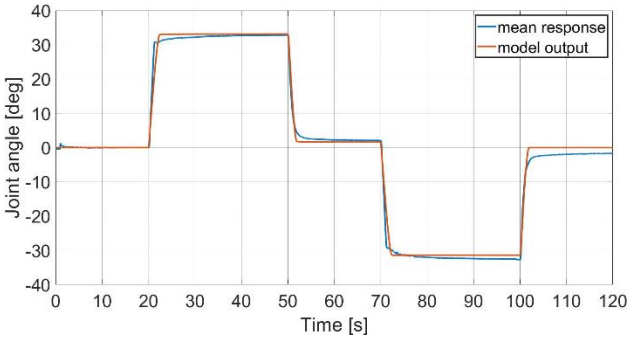

Figure 16. Complete model output of validation for the Link 1

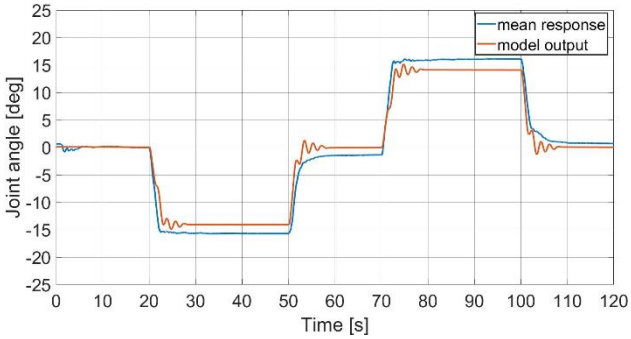

Figure 17. Complete model output of validation for the Link 2

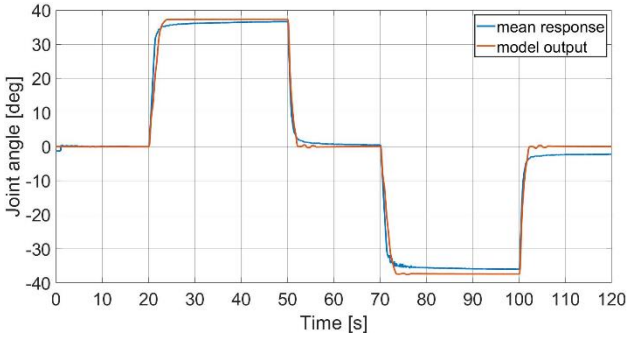

Figure 18. Complete model output of validation for the Link 3

6 CONCLUSIONS

The subject of research in the given article was the complete dynamic characterization of an angular robotic arm with three rotary joints driven by pneumatic artificial muscles. The goal was the creation of a complete dynamic model and its implementation in the Matlab Simulink environment, for the purpose of validation based on measured data from a real system. We used the Lagrangian formalism to derive the dynamics of the links movement. When describing the pneumatic part, we used the parallel nonlinear spring-damper analogy to derive the mechanical part of the pneumatic artificial muscle model and the Boyle-Mariott law to derive the nonlinear differential equations describing the pressure dynamics in the muscle. The subject of the research was obtaining representative courses of the angle of rotation of individual Links based on the measurements. Finally, compare the simulation outputs and the average measured waveforms based on the statistical indicators NRMSE (Normal Root Mean Square Error) and MAE (Mean Absolute Error).

The results of muscle dynamics validation show that for the NRMSE statistical indicator, the highest value was 91.14% for the left muscle of Link 3 and the lowest was 86.93% for the right muscle of Link 2. On average, the value is around 90%. The limit values for the MAE indicator were 5.2831 for the left muscle of Link 1, representing the best value, and 9.3672 for the right muscle of Link 2, representing the worst value. From the point of view of the validation of the complete model of the investigated system, we achieved the best values of the relevant statistical indicators for Link 1, namely NRMSE equal to 93.33% and MAE representing a value of 1.0046. On the other hand, we achieved the worst values for Link 2, for NRMSE it was 82.02% and MAE was 1.4564. Taking into account the presented results, the dynamic model of the experimental manipulator sufficiently describes the behavior of the real system under specific conditions.

ACKNOWLEDGMENTS

The research work is supported by grant VEGA 1/0700/20 „Object Recognition Techniques with Convolutional Neural Networks", by grand KEGA 055TUKE-4/2020 „Transfer of knowledge from research on digitization of production processes into study programs of the Faculty of Manufacturing Technologies" and by grant APVV-19-0590 „Modular Multifunctional Inspection Workplace using Computational Intelligence Techniques".

REFERENCES

[Al-Shuka 2019] Al-Shuka, H. F. N., et al. Dynamics of biped robots during a complete gait cycle: Euler-Lagrange vs. Newton-Euler formulations. School of Control Science and Engineering, Shandong University, Research Report, 2019.

[Albu-Schaffer 2016] Albu-Schaffer, A., Bicchi, A. Actuators for Soft Robotics. In: Springer Handbook of Robotics. Berlín: Springer-Verlag, 2016. ISBN 978-3-319-32550-7.

[Ashagrie 2021] Ashagrie, A., et al. Modeling and control of a 3-DOF articulated robotic manipulator using self-tuning fuzzy sliding mode controller. Cogent Engineering, July 2021, Vol. 8, no. 1, pp. 33.

[Awad 2015] Awad, M., Khanna, R. Efficient Learning Machines. Berkeley: Apress, 2015. ISBN 978-1-4302-5989-3.

[Azar 2022] Azar, A. T., et al. Fractional-Order Euler–Lagrange Dynamic Formulation and Control of Asynchronous Switched Robotic Systems. In: Proceedings of Third International Conference on Sustainable Computing, Jaipur, March 2021. Warszawa: Polish Academy of Sciences, pp. 479-490. ISBN 978-981-16-4537-2.

[Beater 2007] Beater, P. Pneumatic drives: System design, modelling and control. New York: Springer, 2007. ISBN 978-3-540-69470-0.

[Hosovsky 2016] Hosovsky, A., et al. Dynamic characterization and simulation of two-link soft robot arm with pneumatic muscles. Mechanism and Machine Theory, September 2016, Vol. 103, pp. 98-116.

[Kalita 2022] Kalita, B., et al. A Review on the Development of Pneumatic Artificial Muscle Actuators: Force Model and Application. Actuators, October 2022, Vol. 11, no. 10, pp. 1-28.

[Kelly 2005] Kelly, R., et al. Control of Robot Manipulators in Joint Space. London: Springer 2005. ISBN 978-1-85233-994-4.

[Kurfes 2018] Kurfess, T. R. Robotics and Automation Handbook. USA: CRC Press, 2018. ISBN 0-8493-1804-1.

[Lei 2021] Lei, H., et al. Dynamic and Friction Parameters of an Industrial Robot: Identification, Comparison and Repetitiveness Analysis. Robotics, March 2021, Vol. 10., No. 1., pp. 1-17.

[Liu 2015] Liu, Y., et al. Experimental comparison of five friction models on the same test-bed of the micro stick-slip motion system. Mechanical Sciences, March 2015, Vol. 6, No. 1., pp. 15-28.

[Mirvakili 2018] Mirvakili, S., Hunter, I. W. Artificial Muscles: Mechanisms, Applications, and Challenges. Advanced Materials, December 2017, Vol. 30, No. 6, pp. 1-28.

[Murray 1994] Murray, R. M., et al. A Mathematical Introduction to Robotic Manipulation. Boca Raton: CRC Press, 1994.

[Pitel 2013] Pitel, J., Tothova, M. Dynamic Modelling of PAM Based Actuator Using Modified Hill´s Muscle Model. In: Proceedings of the 2013 14th International Carpathian Control Conference (ICCC), Rytro, 26-29, May, 2013. Danwers: IEEE, pp. 307-310, ISBN 978-1-4673-4490-6.

[Siciliano 2016] Siciliano, B. Khatib, O. Springer Handbook of Robotics. Cham: Springer International Publishing, 2016. ISBN 978-3-319-32550-7.

[Spong 2020] Spong, M. V., et al. Robot Modeling and Control. USA: John Wiley&Sons, 2020. ISBN 978-1-119-52399-4.

[Tipler 2004] Tipler, P., Mosca, G. Physics for Scientists and Engineers. New York, W. H. Freeman and Company, 2007. ISBN 978-1-4292-0265-7.

[Trojanova 2020] Trojanova, M., Cakurda, T. Validation of the dynamic model of planar robotic arm with using gravity test. MM Science Journal, December 2020, Vol. 2020, no. December, pp. 4210–4215.

[Trojanova 2021] Trojanova, M., et al. Estimation of Grey-Box Dynamic Model of 2-DOF Pneumatic Actuator Robotic Arm Using Gravity Tests. Applied Sciences, May 2021, Vol. 11, pp. 1-28.

CONTACTS

Ing. Tomas Cakurda, Ing. Monika Trojanova, PhD., Assoc. Prof. Ing. Alexander Hosovsky, PhD.
Technical University of Kosice, Faculty of Manufacturing Technologies with the Seat in Presov, Department of Industrial Engineering and Informatics, Bayerova 1, 080 01 Prešov, Slovakia +421 055 602 6420, tomas.cakurda@tuke.sk, monika.trojanova@tuke.sk, alexander.hosovsky@tuke.sk, http://www.fvt.tuke.sk